Shap. Mem. Superelasticity (2021) 7:179–189
https://doi.org/10.1007/s40830-021-00319-0

TECHNICAL ARTICLE

Valence Electron Ratio for Design of Shape Memory Alloys with Desired Phase Transformation Temperatures

Mehrdad Zarinejad[1] · Kiyohide Wada[2] · Farshid Pahlevani[3] · Reza Katal[4] · Sajjad Rimaz[5]

Received: 14 February 2021 / Revised: 6 March 2021 / Accepted: 9 March 2021 / Published online: 25 March 2021

Abstract Dependence of phase transformation temperatures of TiPd- and TiPt-based shape memory alloys on valence electron ratio (VER), number (e_v/a), and average atomic number of the alloys (Z) are investigated. The alloys have medium numbers of valence electrons ($6.6 \leq e_v/a \leq 7.3$) that are near 7 and a wide range of the average atomic number (Z = 25–54). The forward and reverse phase transformation temperatures, M_s and (A_s), increase with average atomic number of the alloys, respectively. Clear correlations between transformation temperatures and VER are found. M_s and (A_s) both decrease from around 1184 °C (1175 °C) to as low as 20 °C (32 °C), respectively, with increasing VER from 0.134 to 0.270. Temperature hysteresis of the thermoelastic transformation in these alloys tends to decrease with increasing VER. Dependence of transformation temperatures and temperature hysteresis of these shape memory alloys on VER is discussed based on the variations of elastic moduli and atomic bonding due to composition change.

Keywords Phase transformation temperature · Valence electron · Shape memory alloy · TiPd · TiPt · Intermetallics

✉ Mehrdad Zarinejad
mkfalzar@gmail.com

[1] Agency for Science Technology and Research (A*STAR), Singapore Institute of Manufacturing Technology, 2 Fusionopolis Way, Singapore 138634, Singapore

[2] Faculty of Science and Engineering, Swansea University, Bay Campus, Fabian Way, Crymlyn Burrows, Swansea SA1 8EN, UK

[3] Centre for Sustainable Materials, School of Materials Science and Engineering, University of New South Wales, Kensington Campus, High Street, UNSW, Sydney, NSW 2052, Australia

[4] Green Li-ion, 46 Kim Yam Rd, 01-05, Singapore 239351, Singapore

[5] Department of Chemical and Biomolecular Engineering, National University of Singapore, 4, Engineering Drive, Singapore 117585, Singapore

Introduction

There is an ongoing demand for high-temperature shape memory alloys (SMAs) as novel applications continue to be developed in the areas of designing mechanical and aerospace SMA-actuated structures for better system performance. TiPd and TiPt intermetallic systems are among the high-temperature alloys of high interest. To adjust the shape memory and mechanical properties of these intermetallics, alloying elements are added to these systems that alter their transformation temperatures. Phase Transformation temperature of an SMA is an important characteristic, since it is the temperature at which the SMA material recovers from apparent permanent deformation through a reversible martensitic transformation. This shape recovery behavior is often referred to as the shape memory effect and has been adapted in various aerospace, structural, and biomedical applications [1]. Elastic properties of the matrix crystal before martensitic transformation and microstructural features such as precipitates were shown to be important factors affecting the transformation temperatures [2]. To understand the factors that control the transformation temperatures in the SMAs system, Zarinejad and Liu suggested the need to acquire in-depth knowledge of how the atomic bonding strength of the matrix crystal can be influenced by the chemical composition of the alloys. Dependence of transformation temperatures on electron

variables in SMAs was introduced [3–5]. It was shown that variation of elastic properties of the parent crystal (austenite) because of composition change influence the resistance against shear, responsible for martensitic phase transformation. This understanding was achieved based on the knowledge that prior to martensitic transformation a softening of elastic moduli occurs with the lowering temperature. The experimental results, mainly in Cu-based and NiTi-based SMAs [6–9], suggest that there is a critical value of elastic constant at which transformation takes place, which is not sensitive to alloy compositions [10], and is only slightly dependant on temperature [2]. Based on this, the elastic moduli of the alloy, which are dependent on both composition and temperature are the key parameters influencing the transformation temperatures, [2, 11]. Since in metallic materials the delocalized valence electrons dominate the strengths of bonds and elastic properties [12–14], it is of particular importance to study the electronic parameters of alloys.

In the present work, the investigation is extended to the vast TiPd-based and TiPt-based high-temperature SMA family of alloys in detail to reveal in-depth understanding of the dependence of transformation temperatures (M_s, A_s) on the electronic parameters of the alloy. The electronic parameters of nearly all the TiPd-based and TiPt-based alloys made or studied to date are examined. Three parameters are paid attention to in the current study: (1) the average atomic number of the alloys; (2) the number of valence electrons, and; (3) Valence Electron Ratio (VER) of the alloys.

We reveal and explain the dependence of the transformation temperatures of important TiPd and TiPt family of alloys on VER. The correlations found in the current work enable an important understanding towards effective alloy design.

Materials and Methods

Different Ti/Pd or Ti/Pt atomic ratios and alloying elements such as Ni, Fe, Co, Cr, Mn, Cu, V, Hf, W, Ta, Ir, etc., have been utilized by researchers to alter the transformation temperatures and characteristics of TiPd and TiPt SMAs. A survey of the literature reveals many TiPd- and TiPt-based shape memory alloys was performed to extract the phase transformation temperatures and temperature hysteresis. The data [14–64] were extracted from the relevant literature as listed in tables or presented in graphs. Almost all the data correspond to solution-treated alloys to minimize the effects of precipitates and mechanical work. These possible effects, if existing, were not considered in the present work. The average atomic numbers of the alloys were calculated based on the atomic fractions and atomic numbers of the elements comprising the alloys as follows:

$$Z = f_{\mathrm{Ti}} Z_{\mathrm{Ti}} + f_{\mathrm{Pd(Pt)}} Z_{\mathrm{Pd(Pt)}} + f_{\mathrm{T}} Z_{\mathrm{T}} + f_{\mathrm{Q}} Z_{\mathrm{Q}} \quad (1)$$

where Z is the fraction-averaged atomic number of the alloy. Z_{Ti}, $Z_{\mathrm{Pd(Pt)}}$, Z_{T}, and Z_{Q}, etc. are the atomic numbers Ti, Pd (or Pt), the ternary, quaternary, quinary elements and so on, respectively. The f_x (x = Ti, Pd or Pt, the ternary, quaternary, quinary elements, or even quinary element, etc.) is the corresponding atomic fraction of each element in the alloy. To study the dependence of the transformation temperatures on the chemistry of alloys the basic electron configurations of the alloys were analyzed in the following section.

The number of valence electrons is usually considered as the number of *d* and *s* electrons for an atom of transition metals. The valence electrons per atom of TiPd- and TiPt-based alloys can be calculated based on the atomic fractions of the elements in the alloy by the following equation:

$$\frac{e_{\mathrm{v}}}{a} = f_{\mathrm{Ti}} e_{\mathrm{v}}^{\mathrm{Ti}} + f_{\mathrm{Pd(Pt)}} e_{\mathrm{v}}^{\mathrm{Pd(Pt)}} + f_{\mathrm{T}} e_{\mathrm{v}}^{\mathrm{T}} + f_{\mathrm{Q}} e_{\mathrm{v}}^{\mathrm{Q}} + \cdots \quad (2)$$

where similarly f_{Ti}, $f_{\mathrm{Pd(Pt)}}$, f_{T} and f_{Q} represent the atomic fractions of Ti, Pd (or Pt), the ternary quaternary elements, etc., in the alloy and, $e_{\mathrm{v}}^{\mathrm{Ti}}$,$e_{\mathrm{v}}^{\mathrm{Pd(Pt)}}$,$e_{\mathrm{v}}^{\mathrm{T}}$ and $e_{\mathrm{v}}^{\mathrm{Q}}$ are the corresponding numbers of valence electrons of elements Ti, Pd (Pt), ternary and quaternary elements, respectively. The valence electron ratios (VER) of the alloys were calculated. VER is defined as the ratio of the number of valence electrons to the total number of electrons of the alloy, VER = (e_{v}/e_{t}), which can be simply calculated as follows:

$$\mathrm{VER} = \frac{e_{\mathrm{v}}}{e_{\mathrm{t}}} = \frac{f_{\mathrm{Ti}} e_{\mathrm{v}}^{\mathrm{Ti}} + f_{\mathrm{Pd}} e_{\mathrm{v}}^{\mathrm{Pd(Pt)}} + f_{\mathrm{T}} e_{\mathrm{v}}^{\mathrm{T}} + f_{\mathrm{Q}} e_{\mathrm{v}}^{\mathrm{Q}}}{f_{\mathrm{Ti}} Z_{\mathrm{Ti}} + f_{\mathrm{Pd(Pt)}} Z_{\mathrm{Pd(Pt)}} + f_{\mathrm{T}} Z_{\mathrm{T}} + f_{\mathrm{Q}} Z_{\mathrm{Q}}} \quad (3)$$

where $Z_{\mathrm{Ti,}}$ $Z_{\mathrm{Pd,(Pt)}}$ $Z_{\mathrm{T,}}$ Z_{Q} etc., represent the atomic numbers of Ti, Pd (Pt), the ternary and quaternary elements, etc., respectively. Similarly f_{Ti}, $f_{\mathrm{Pd(Pt)}}$, f_{T}, f_{Q} represent their corresponding atomic fractions in the alloy.

Theory (Elastic Properties of Crystal and Phase Transformation)

In the martensitic transformation in TiPd- and TiPt-based alloys shear causes shape changes to the austenite parent crystals. The elastic response coefficients are the most fundamental of all the properties of solid crystals and the most important subset of them are the shear and bulk moduli. Bulk modulus is a measure of the resistance of a solid to volume change and shear modulus is a measure of resistance to shape change. Shear moduli have the highest influence on the mechanical properties of the crystals

[1, 2, 9, 65]. Bonding type (metallic, covalent, ionic, and molecular), and solidity index of a crystal (which is simply the ratio of the shear modulus to the bulk modulus, multiplied by a coefficient of the order of unity), have been used to classify crystals [12, 65]. Therefore, shear and bulk moduli and their ratio in the parent phase (austenite) are of paramount importance for this athermal martensitic phase transformation [2, 65]. The chemical factors that affect these parameters in the TiAu- and TiIr-based alloys under study in this work are discussed in the following.

Results and Discussion (Chemical Factors Influencing Bulk and Shear Moduli of Alloy Crystals)

Average Atomic Number

Table 1 presents more than 120 TiPd and TiPt alloy compositions [2, 14–64] that include nearly all alloy compositions studied so far, together with their forward and reverse transformation temperatures (M_s and A_s) in ascending order, and the thermal hysteresis where available. The maximum martensite start temperature (M_s = 713 °C) for TiPd-based system corresponds to a Pt and Zr alloyed composition, i.e., $Ti_{45}Zr_5Pd_5Pt_{45}$, whereas in the TiPt system, Ir-alloyed compositions exhibit the highest M_s temperatures, with $Ti_{50}Pt_{12.5}Ir_{37.5}$ having a M_s of 1184 °C. The lowest transformation temperatures correspond to alloys with minimum Pd or Pt quantity in their compositions.

The average atomic numbers of the alloys under study are tabulated in Table 1. The transformation temperatures of these alloys clearly increase with Z of the alloys, as plotted in Fig. 1. The transformation temperature in the alloy systems studied shows increasing trends with the increasing average atomic number of the alloys (Fig. 1). In transition metals and intermetallics it is known that when the average atomic number is halfway through in the transition metals rows of the periodic table of elements, i.e., either $Z = 25$–26, or $Z = 43$–44, and so on., the martensitic transformation temperature can be reduced to some extent. This is because the elastic properties of the parent crystal hit maxima at or near these atomic numbers [65], and martensitic transformation should start at a lower temperature. This effect (if present) is masked by data scatter in the current work (Fig. 1). As shown, the existing TiPt alloys can have higher transformation temperatures than TiPd alloys, though the trend of change of M_s and A_s temperatures with atomic number is similar. These temperatures increase with the increasing atomic number of the alloys. In other words, the transformation temperatures of the alloys increase with increasing the total number of electrons (average atomic number) of the alloy. Non-valence electrons do not contribute to bonding and together with the protons comprise the ion kernel in the metallic bonding of the transition metal alloys. Increasing the non-valence electrons or the size of the kernels at constant (or nearly constant) valence electron numbers leads to weaker elastic bonding [65, 66]. This, in turn, means the resistance to shape and volume change of the crystal will be lower (at least in some crystallographic directions), and therefore, the phase change from austenite to martensite may occur at higher temperatures. The presence of Pt ($Z = 78$) and Pd ($Z = 46$) in the alloys causes the total number of non-valence electrons to extensively increase, with the influence of the former more than the latter due to higher Z (Table 1).

Number of Valence Electrons

Alloys with M_s (A_s) temperatures from as high as 1184 (1175) °C down to 20 °C (32 °C) were included in this investigation. In the categorization of the shape memory alloys (SMAs) with respect to their number of valence electrons per atom, a wide range was previously observed ($4 \leq e_v/a \leq 12$) by Zarinejad and Liu [5]. The alloys were divided into low ($e/a < 5$), medium ($5 \leq e/a \leq 7.50$) and high ($e/a > 7.50$) valence electron groups. On this basis, TiPd-, and TiPt-based alloys all belong to the medium valence electron group with their e/a (6.65–7.30) in a range equal to or near 7 (Table 1). A considerable number of non-magnetic SMAs happen to belong to the medium range [5]. Majority of the highest M_s in shape memory alloy systems are usually observed in the medium electron group ($5 \leq e_v/a \leq 7.50$) [5], especially when e_v/a is 7.00 or near 7.00 ($6.6 \leq e_v/a \leq 7.3$). A wide scatter of M_s temperatures of the alloys in this narrow range of valence electron per atom is observed (Fig. 2a). Similarly, a scatter of austenite start temperatures, A_s, with a relatively narrow number of valence electrons per atom variation is observed for (Fig. 2b). A wide range of transformation temperatures is observed, even though in TiPd- and TiPt-based alloy systems, the numbers of valence electrons per atom that contributes to the bonding strengths are close to each other. This indicates that although the number of e_v/a is a factor in bonding, its effect must be studied along with other influencing factors such as the average atomic number (Z). With the increasing number of non-valence electrons because of increasing the average atomic number of the alloys at an almost constant bonding power (valence electrons), the interatomic bonding that keeps the ion kernels in the metallic bonds together is affected by the size and density of the kernels, [4, 65]. Higher numbers of non-valence electrons and protons in this condition reduce the bonding effects of the valence electrons and, therefore, reduce the elastic moduli at least in some shear directions.

Table 1 Martensite start temperature (M_s), Austenite start temperature (A_s), temperature hysteresis, number of valence electrons per atom (e_v/a), valence electron, ratio (VER) and average atomic number (Z) of TiPd- and TiPt-based shape memory alloys

Alloy	M_s [°C]	A_s [°C]	Hysteresis [°C]	e_v/a [e/atom]	VER	Z	References
$Ti_{50}Pd_5Ni_{45}$	20	–	–	7	0.27	25.9	[2]
$Ti_{50}Pd_{10}Ni_{40}$	26	32	20	7	0.261	26.8	[14]
$Ti_{54}Pd_{9.2}Ni_{36.8}$	26	32	18	6.76	0.256	26.4	[15]
$Ti_{50.5}Ni_{34.5}Pd_{15}$	73	75	10	6.97	0.252	26.7	[16]
$Ti_{51}Pd_{20}Ni_{29}$	85	–	–	6.94	0.243	26.8	[17]
$Ti_{48}Ni_{27}Pd_{25}$	88	96.7	–	7.12	0.241	29.6	[18]
$Ni_{40}Ti_{50}Pt_{10}$	90	100	–	7	0.244	28	[19]
$Ti_{51}Pd_{22.5}Ni_{26.5}$	95	–	–	6.94	0.239	28.5	[20]
$Ti_{45.5}Ni_{24.5}Pd_{25}Ta_5$	105.4	121.6	29.8	7.02	0.22	32	[21]
$Ni_{25.3}Ti_{49.7}Pd_{25}$	117	122	12	7.02	0.24	29.3	[22]
$Ti_{50}Pd_{40}Mn_{10}$	118	–	–	6.7	0.211	31.9	[23]
$Ti_{50}Pd_{20}Ni_{30}$	123	110	17	7	0.233	30	[24]
$Ti_{50}Pd_{22}Ni_{27}W_1$	132.3	130.8	32.2	6.96	0.236	28.6	[25]
$Ni_{24.3}Ti_{49.7}Pd_{26}$	134	150	–	7.02	0.236	29.7	[26]
$Ti_{50}Pd_{24}Ni_{25}W_1$	138.8	114.7	25.1	6.96	0.234	29.4	[25]
$Ti_{50.2}Ni_{24.8}Pd_{25}$	151.6	172.5	–	6.98	0.236	29.5	[27]
$Ti_{50}Ni_{20}Pd_{25}Cu_5$	155	156	–	7.05	0.238	29.6	[28]
$Ni_{25}Ti_{50}Pd_{25}$	157	169	7	7	0.237	29.5	[22]
$Ni_{24.7}Ti_{49.3}Pd_{25}Sc_1$	161	152	10	6.97	0.236	29.5	[29]
$Ti_{50}Pd_{38}Co_{12}$	169	–	–	6.88	0.217	31.7	[23]
$Ti_{50}Ni_{15}Pd_{25}Cu_{10}$	170	179	–	7.1	0.239	29.6	[28]
$Ti_{50}Ni_{24.5}Pd_{25}Sc_{0.5}$	170.1	177.6	–	6.96	0.235	29.5	[27]
$Ti_{50}Pd_{25}Ni_{24}W_1$	177	168	15	6.96	0.232	29.8	[25]
$Ti_{50}Pd_{40}Fe_{10}$	177	–	–	6.8	0.214	30	[30]
$Ni_{24.7}Ti_{50.3}Pd_{25}$	179	193	10	6.98	0.237	29.5	[29]
$Ti_{49.5}Ni_{24.5}Pd_{25}Ta_1$	179.1	188.5	23.2	6.98	0.233	30	[21]
$Ti_{50.5}Ni_{24.5}Pd_{25}$	179.4	184.1	–	6.97	0.236	29.5	[27]
$Ti_{50}Ni_{25}Pd_{25}$	182	193	–	7	0.237	29.5	[31]
$Ti_{51.2}Pd_{27.0}Ni_{21.8}$	187	–	–	6.93	0.233	32	[32]
$Ti_{50.5}Ni_{24.5}Pd_{25}$	190	193	7	6.97	0.236	29.5	[16]
$Ti_{50}Ni_{15}Pd_{25}Cu_{10}$	192	205	–	7.1	0.239	29.6	[31]
$Ti_{50}Pd_{30}Ni_{20}$	192	203	25	7	0.23	29.8	[14]
$Ni_{24.7}Ti_{50.3}Pd_{25}$	192	193	8	6.98	0.236	29.5	[29]
$Ti_{50}Pd_{43}Mn_7$	197	–	–	6.79	0.209	30.4	[30]
$Ti_{50}Ni_{10}Pd_{25}Cu_{15}$	203	204	–	7.15	0.239	29.8	[28]
$Ti_{50}Pd_{42}Fe_8$	206	–	–	6.84	0.211	32.4	[23]
$Ti_{50}Pd_{25}Ni_{25}$	207	177	20	7	0.237	32.5	[33]
$Ti_{49.5}Pd_{28.5}Ni_{22.0}$	207	–	–	7.03	0.233	29.5	[32]
$Ti_{50}Pd_{35}Ni_{15}$	225	–	–	7	0.223	30.2	[17]
$Ti_{40}Pd_{50}Zr_{10}$	227	256	–	7	0.195	35.8	[34]
$Ti_{54}Ni_{16}Pd_{30}$	240	236	30	6.76	0.224	30.2	[35]
$Ti_{50}Pd_{30}Ni_{20}$	242.4	253.1	37.8	7	0.23	31.1	[36]
$Ni_{19.5}Pd_{30}Ti_{50.5}$	249	256	11	6.97	0.229	30.4	[37]
$Ti_{50}Pd_{45}Cr_5$	257	–	–	6.8	0.207	32.9	[30]
$Ti_{50}Pd_{32}Ni_{18}$	257	–	–	7	0.227	30.8	[30]
$Ti_{52.03}Pt_{18.50}Ni_{29.01}$	259	268	–	6.83	0.201	28.1	[20, 38]
$Ni_{30}Ti_{50}Pt_{20}$	266	271	31	7	0.2	35	[39]
$Ti_{50}Pd_{45}V_5$	277	–	–	6.94	0.208	32.8	[30]
$Ti_{50}Pd_{43}Fe_7$	327	–	–	6.84	0.211	32.6	[30]

Table 1 continued

Alloy	M_s [°C]	A_s [°C]	Hysteresis [°C]	e_v/a [e/atom]	VER	Z	References
$Ti_{50}Pd_{46}In_4$	327	–	–	6.72	0.197	34.1	[40]
$Ti_{45}Pd_{20}Ni_{10}Pt_{20}Zr_5$	337	374	105	7	0.178	39.5	[41]
$Ti_{50}Pd_{46}Cr_4$	342.3	347.55	22.47	6.84	0.209	32.8	[42]
$Ti_{50.5}Ni_{28.5}Pt_{21}$	344.6	327	–	6.97	0.197	35.4	[27]
$Ti_{50}Pd_{37}Ni_{13}$	350	–	–	7	0.221	31.7	[43]
$Ti_{43.53}Pd_{50}Hf_{6.47}$	355	–	–	7	0.188	37.2	[44]
$Ti_{54}Ni_{26}Pt_{20}$	361	367	48	6.76	0.194	34.8	[35]
$Ti_{50}Pd_{40}Ni_{10}$	383	448.5	69.5	7	0.217	32.2	[45]
$Ti_{50}Pd_{40}Ni_{10}$	390	400	28	7	0.217	32.2	[46]
$Ti_{54}Ni_6Pd_{40}$	391	401	46	6.76	0.212	32	[35]
$Ti_{45}Pd_{50}Zr_{2.5}V_{2.5}$	393	523	–	7.02	0.204	34.5	[47]
$Ti_{50}Pd_{40}Ni_{10}$	398.5	414.3	42.2	7	0.217	32.2	[36]
$Ti_{50}Pd_{42}Ni_8$	400	–	–	7	0.214	32.8	[30]
$Ni_{25}Ti_{50}Pt_{25}$	436.4	448.8	49.1	7	0.187	37.5	[20]
$Ti_{50}Pd_{44}Co_6$	417	–	–	6.94	0.211	32.7	[30]
$Ti_{43}Pd_{50}Zr_7$	421	451	–	7	0.199	35.2	[47]
$Ti_{45}Zr_5Pd_{45}Ir_5$	422	457	53	6.95	0.191	36.4	[48]
$Ti_{45}Pd_{50}Zr_1V_4$	441	496	–	7.04	0.208	33.9	[47]
$Ti_{54}Pd_{43}Ni_3$	447	452	65	6.76	0.208	32.5	[35]
$Ti_{50}Pd_{38}Ir_{12}$	452	471	56	6.88	0.185	37.3	[49]
$Ti_{45}Pd_{50}Zr_5$	457	466	–	7	0.2	34.9	[34]
$Ti_{50}Pd_{45}Ni_5$	457	518	51	7	0.211	33.1	[45]
$Ti_{50}Pd_{42}Ir_8$	479	478	43	6.92	0.19	36.5	[49]
$Ti_{50}Pt_{27.5}Ni_{22.5}$	480	500	–	7	0.18	38.7	[38]
$Ti_{50.5}Ni_{3.5}Pd_{46}$	485	509	28	6.97	0.209	33.2	[16]
$Ti_{45}Pd_{20}Ni_5Pt_{25}Zr_5$	502	520	40	7	0.167	42	[41]
$Ti_{49.82}Pd_{50}Hf_{0.18}$	505	537	–	7	0.205	33.9	[44]
$Ti_{50}Pd_{50}$	510	520	40	7	0.205	34	[34, 50]
$Ti_{50}Pd_{50}$	510	520	70	7	0.205	34	[51]
$Ti_{50}Pt_{29}Ni_{21}$	510	530	–	7	0.177	39.5	[38]
$Ti_{50}Pt_{30}Ni_{20}$	514	552	–	7	0.205	30.4	[20]
$Ti_{50}Pd_{50}$	514	552	55	7	0.205	34	[14]
$Ni_{35}Ti_{30}Pd_{15}Hf_{20}$	525	537	–	7	0.186	37.7	[52]
$Ti_{55}Pd_{45}$	527	580	50	6.7	0.204	32.8	[53]
$Ti_{50}Pd_{50}$	527	568	–	7	0.205	34	[34]
$Ti_{50}Pd_{50}$	534	605	–	7	0.205	34	[54]
$Ti_{50}Pd_{50}$	537	–	–	700	0.205	34	[40]
$Ti_{50}Pd_{50}$	537	587	55	7	0.205	34	[53]
$Ti_{50}Pd_{50}$	544.7	574	46.1	7	0.205	34	[55]
$Ni_{20.2}Ti_{49.8}Pt_{30}C_{0.2}$	560	594	55	7.02	0.175	40	[39]
$Ni_{20}Ti_{49.4}Pt_{29.8}C_{0.8}$	562	568	35	6.99	0.175	39.8	[39]
$Ni_{20.79}Ti_{47.79}Pt_{30.79}$	605	666	114	7.07	0.175	40.3	[20]
$Ni_{25}Ti_{25}Pd_{25}Hf_{25}$	630	690		7	0.167	42	[52]
$Ni_{18}Ti_{50}Pt_{32}$	630	670	–	7	0.171	41	[20]
$Ni_{15}Ti_{50}Pt_{35}$	680	750	–	7	0.165	42.5	[20]
$Ni_{25}Pd_{25}Ti_{16.7}Hf_{16.7}Zr_{16.7}$	690	720	–	7	0.171	40.9	[52]
$Ti_{45}Zr_5Pd_{15}Pt_{35}$	713	725	91	7	152	46.1	[50]
$Ni_{12}Ti_{50}Pt_{38}$	750	780	–	7	0.159	44	[20]
$Ti_{45}Zr_5Pd_5Pt_{45}$	774	896	112	7	0.142	49.3	[56]

Table 1 continued

Alloy	M_s [°C]	A_s [°C]	Hysteresis [°C]	e_v/a [e/atom]	VER	Z	References
$Ni_{10}Ti_{50}Pt_{40}$	810	850	–	7	0.156	45	[20]
$Ti_{40}Pt_{50}Zr_{10}$	865	926		7	0.136	51.8	[57]
$Ti_{50}Pt_{43.75}V_{6.25}$	889	1005		6.65	0.147	46.6	[58]
$Ti_{45}Pt_{50}Zr_5$	897	939	–	7	0.138	50.9	[59]
$Ti_{50}Pt_{45}Co_5$	907	957	–	6.95	0.146	47.5	[57]
$Ni_8Ti_{50}Pt_{42}$	910	960		7	0.152	46	[20]
$Ti_{50}Pt_{45}Ru_5$	912	917	–	6.9	0.143	48.3	[60, 61]
$Ti_{50}Pt_{45}Ru_5$	913	925	95	6.9	0.143	48.3	[59]
$Ti_{45}Pt_{50}Hf_5$	915	–	60	7	0.134	52.5	[62]
$Ti_{50}Pt_{45}Ru_5$	925	–	–	6.9	0.143	48.3	[62]
$Ti_{50}Pt_{50}$	974	1025		7	0.14	50	[58]
$Ti_{55}Pt_{45}$	975	1010		7.3	0.139	47.2	[63, 64]
$Ti_{44}Pt_{56}$	980	1020	–	7.36	0.138	53.3	[63]
$Ti_{50}Pt_{50}$	989	1000	94	7	0.14	50	[48, 61]
$Ti_{50}Pt_{50}$	992	997	–	7	0.14	50	[48, 61]
$Ti_{53}Pt_{47}$	995	1035	–	6.82	0.142	48.3	[63, 64]
$Ti_{50}Pt_{37.5}Ir_{12.5}$	1000	1036	103	6.88	0.138	49.9	[61]
$Ti_{50}Pt_{50}$	1020	1040	–	7	0.14	50	[63, 64]
$Ti_{50}Pt_{50}$	1020	1045	–	7	0.14	50	[61]
$Ti_{55}Pt_{45}$	1025	1030	55	6.7	0.142	47.2	[64]
$Ti_{50}Pt_{50}$	1025	1045	55	7	0.14	50	[61, 63]
$Ti_{49}Pt_{51}$	1030	1050	–	7.06	0.139	50.5	[63]
$Ti_{50}Pt_{45}Ir_5$	1040	–	48	6.95	0.139	49.95	[62]
$Ti_{49.5}Pt_{50.5}$	1065	1040	–	7.03	0.14	50.2	[64]
$Ti_{50}Pt_{50}$	1070	1040	65	7	0.14	50	[48, 51]
$Ti_{50}Pt_{25}Ir_{25}$	1110	1121	80	6.75	0.136	49.8	[48, 51]
$Ti_{50}Pt_{20}Ir_{30}$	1145	1159	44	6.7	0.135	49.7	[48, 51]
$Ti_{50}Pt_{12.5}Ir_{37.5}$	1184	1175	34	6.63	0.134	49.6	[48, 51]

The references show the sources of transformation temperatures and hysteresis data

Valence Electron Ratio (VER) and Transformation Temperatures

Depending on the alloying elements, atomic fractions of elements comprising an alloy, different VER values have resulted. These values for the alloys examined are tabulated in Table 1. The variations of M_s and A_s temperatures vs. VER are plotted in Fig. 3. In both cases, a main trend is observed with increasing the electron ratio. M_s and A_s both, decrease consistently from temperatures as high as 1184 (1179) °C with VER values as low as 0.134 down to temperatures as low as 20 (32) °C with VER values of as high as 0.270. The general trends of variation of M_s and A_s with VER are similar (Fig. 3). Furthermore, Fig. 4 illustrates the combined influence of VER and e_v on the transformation temperatures. It is evident that the variation of these temperatures with VER is more pronounced and follows a descending trend with increasing VER. The influence of e_v is masked by the dominance of the effect of VER (Fig. 4). The relationship between VER, elastic properties, and transformation temperatures of the alloys are discussed. In metallic bonding, the valence electrons act like 'glue', bonding non-valence electrons and nuclei units together [4, 5, 66]; whereas non-valence electrons contribute to the total atomic volume of the alloy. Increasing VER could mean thickening of the 'glue' bonding the ionic kernels together. An established empirical relationship between the valence electron density and

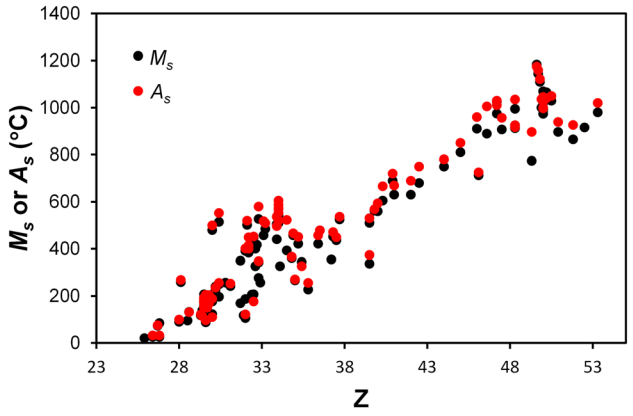

Fig. 1 Transformation temperatures vs. atomic number: variations of Martensite start (M_s) and Austenite start (A_s) temperatures with average atomic number of TiPd- and TiPt-based alloys (Z)

bulk modulus of metallic materials and intermetallic compounds is known. Higher VER usually results in higher bulk and, therefore, higher shear moduli [65, 66]. Increasing VER of the TiPd-based and TiPt-based alloys, therefore, is expected to result in higher elastic and shear moduli. The change of VER by replacing alloying elements for Ti, and Pd (Pt) is accompanied by a change in the elastic properties as the interatomic bonding is affected. A key factor controlling the bonding is the VER of the alloy. Before the martensitic transformation, the elastic moduli decrease during cooling and reach a critical value in a phenomenon known as the pre-curser effect [2]. If the elastic moduli of B2 austenite crystal of these alloys are enhanced because of higher VER, the cooling should continue to lower temperatures before a critical elastic constant is reached because of pre-martensitic softening of bulk and/or shear moduli, hence M_s is decreased. This is

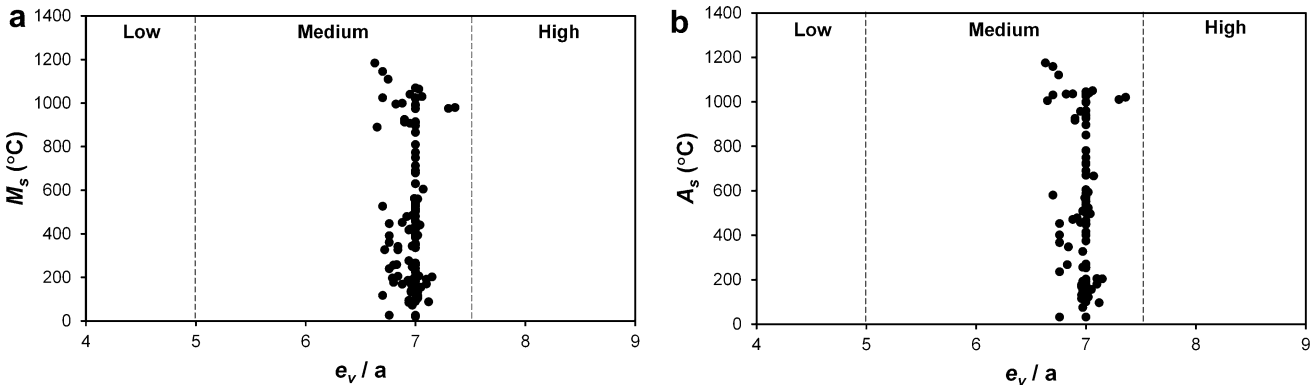

Fig. 2 Transformation temperatures vs. number of valence electrons: variations of M_s and A_s with the number of valence electrons per atom (e_v/a) of TiPd- and TiPt-based alloys: **a** Martensite start (M_s); and **b** Austenite start (A_s) temperatures

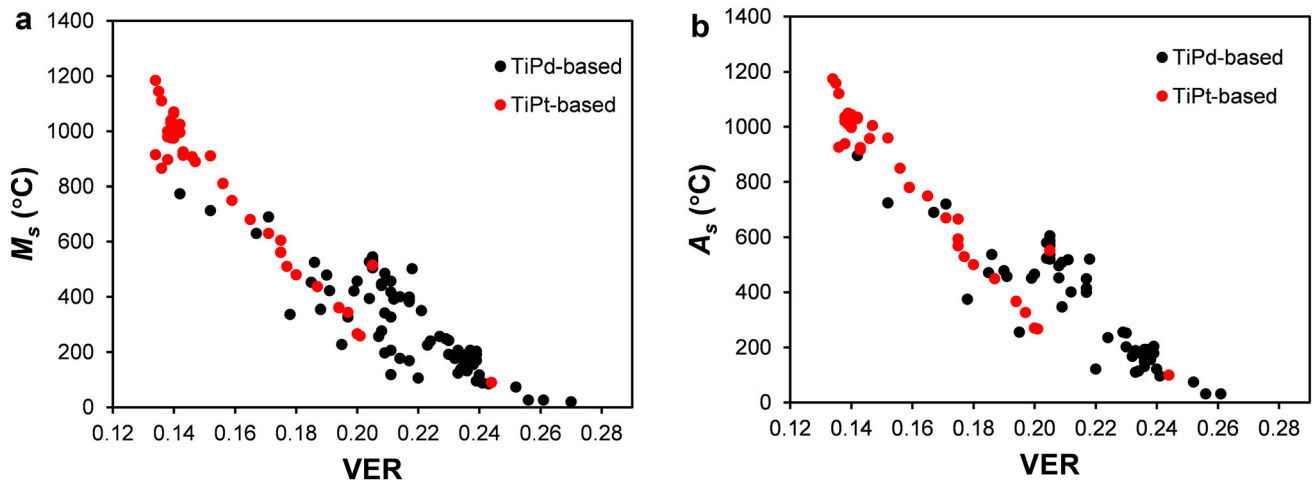

Fig. 3 Transformation temperatures vs. valence electron ratio: dependence of M_s and A_s on the valence electron ratio (VER) of the TiPd- and TiPt-based alloys: **a** Martensite start (M_s); and **b** Austenite start (A_s) temperatures

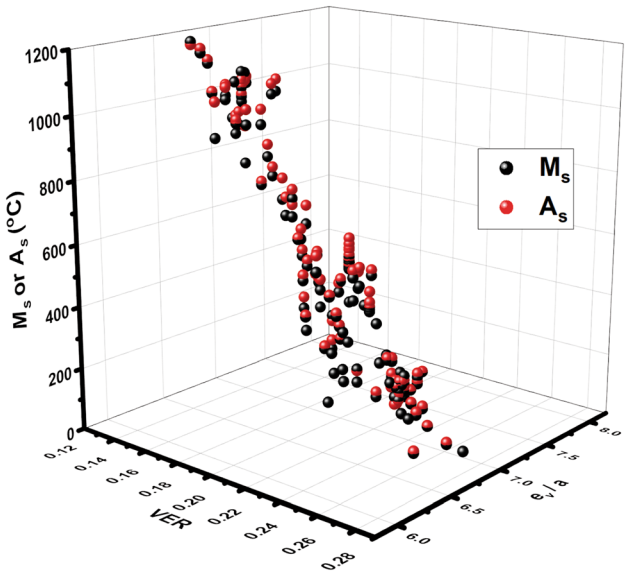

Fig. 4 Transformation temperatures vs. ratio and number of valence electrons: combined influence of valence electron ratio (VER) and number of valence electrons (e_v/a) on M_s and A_s Temperatures of the TiPd- and TiPt-based. The dominance of the influence of VER over e_v can be observed

the case in nearly all alloying elements added in the present alloys that result in the transformation temperatures to reduce from that of the highest M_s alloy to the lowest (Table 1). On the contrary, if the alloy has lower elastic bulk and shear moduli in the austenite phase, the critical elastic constant can be reached at higher temperatures and M_s is increased. Any alloying elements that increase the VER of the alloy, decrease the transformation temperatures. Ni, Cu, Sc, etc. are examples of alloying elements that increase VER and lower the transformation temperatures. In case the addition of the alloying elements results in a reduction of VER, the transformation temperatures are elevated. For instance, the addition of Ir, Pt, Hf, Pd, Hf, etc. reduces the VER of the alloy and elevates the transformation temperatures. Ir and Pt are more effective in the increase of M_s and A_s due to higher Z (Table 1, Figs. 3 and 4). For each shape memory alloy, M_s is determined based on the elastic moduli of austenite and A_s follows M_s due to reversibility of the thermoelastic shape memory alloys in this study. M_s is controlled by VER, and the reverse transformation starting at (A_s) which is necessitated by reduction of the energy of the system due to increased vibrations of electrons and atoms in the crystal (by the increase of the temperature), is influenced by the factors that determine the thermal hysteresis, i.e., relaxation of stress arising from the forward transformation, defect structure changes inherited from the austenite to martensite transformation, or formed during reverse transformation (the level of bonds breakage and fluctuation of VER at dislocations). These factors determine the degree of reversibility of the transformation. Hence A_s (influenced by reversibility factors) follows M_s as the empirical data trend shows (Fig. 3).

These discussions explain why some of the TiPd- and TiPt-based SMA compositions have high, and some others have low transformation temperatures. Moreover, in austenite to martensite transformation in these alloys, where shear is responsible for phase change from cubic to orthorhombic, the change of VER in austenite may affect the shear moduli of the crystals in different directions (C_{44} and C^* as two main shear constants of the austenite B2 cubic crystal) differently, and therefore, the Zener's anisotropy factor $A = C_{44}/C^*$ will be affected by VER [65]. The anisotropy factor in turn facilitates shear and the martensite start temperature to be changed. The shown trends are general and indicative of the major underlying influence of VER on the transformation temperatures.

A comparison of the effect of e_v/a, and VER on transformation temperatures in magnetic and non-magnetic shape memory alloys can be useful. The e_v/a parameter is of paramount importance in all systems of shape memory alloys. However, the level of their influence on the transformation temperature is different and is dependent on: (a) what range of $e_v/$ and VER we are dealing with; and (b) presence or lack of presence of magnetization and antiferromagnetism in the alloys. It was shown that when $5 \leq e_v/a \leq 7.5$, the effect of e_v/a is less pronounced, and VER is dominant [5]. The alloys studied in the present work belong to this category and their transformation temperatures are dominated by VER. In other words, it is the change of VER that controls the transformation temperature and e_v/a is less influential, as shown in Fig. 4. On the other hand, in magnetic shape memory alloys such as Heusler alloys and half Heusler alloys (containing Mn, Cr, Co, etc.), the transformation temperature characteristics are more complicated. Most of the alloys belong to the high valence electron category (e_v/a more than 7.5), although some of them may have an e_v/a parameter of 7–7.5. More Importantly, their VER value is high (VER > 0.27) [5]. In high VER alloys, the number of electrons per atom for bonding seems to be too high and, further increase of it has a negative effect on bonding and in turn on elastic properties of the austenite crystal. As a result, higher e_v/a in these alloys results in increased transformation temperatures. Hybridization of d orbitals with s and p orbitals of common elements in magnetic shape memory alloys such as Ga, In, Al, Sn, etc., also influence the stability of austenite vs. martensite. Moreover, when VER of the alloy is high (VER > 0.27) by increasing the concentrations of elements such as Mn or Cr and possibly some other elements beyond a certain limit the elastic properties of austenite are negatively affected due to the antiferromagnetic behavior that these elements can exhibit and M_s and

A_s temperatures both increases. Magnetization makes austenite more stable and decreases the transformation temperature and anti-ferromagnetism can reduce the strength of the bonds (at least in some shear directions) and make austenite less stable, hence increases the M_s and A_s temperatures.

Therefore, in magnetic shape memory alloys, by increasing e_v/a, because of the excessive amount of valence electrons, the transformation temperatures increase, and its effect is more pronounced and could be a very influential parameter. This is not seen in non-magnetic alloys, where VER plays a dominant role.

The general trend presented in this work provides an overall criterion for the design of the alloys with the desired service temperature. However, comparisons at small differences in temperature or compositions concerning the overall trend is not recommended owing to the scatter of data (Figs. 3 and 4). Details of the microstructural features and deformation regime of the alloy need to be known for comparisons in small differences between the alloys. However, VER seems to be the most influential factor dominating the transformation temperatures.

Temperature Hysteresis

The available data for transformation hysteresis in the alloys under study show a relatively wide range of transformation hysteresis (7–114 °C) (Table 1). It is shown that by increasing the valence electron ratio (VER) of alloys the transformation temperature hysteresis is generally decreased (Fig. 5a). In addition, temperature hysteresis increases with the average atomic number of the alloys, (Z) (Fig. 5b). These are indicative of the influence of the strengths of the bonds in the thermoelastic transformation. However, how the strengths of the bonds affect it, is complex, since hysteresis is dependent on several factors at microstructure, crystal structure, and (electronic) bonding levels. In principle, in alloys and intermetallic compounds, the dislocation mobility is determined by the pattern and intensities of the electron density fluctuations. VER is, to a major extent, in line with the valence electron density of the material as shown by Zarinejad et al. [4, 5]. It can simply be argued that in general, weaker atomic bonds can be plastically strained more extensively, following thermoelastic martensitic transformation. The relaxation of the energy by plastic deformation mechanisms results in wider hysteresis. The strengths of the bonds are controlled by valence electrons among other factors. Based on this argument, the alloys with higher VER and stronger austenite bonds exhibit narrower temperature hysteresis as is seen in this study (Table 1, Fig. 5a). However, the complexity of hysteresis is further realized as it is controlled by other factors at microstructure and atomic scales. In crystals with non-local bonding electrons, where dislocation lines move concertedly (such as in transition metal alloys), the motion of the dislocation lines is not activated. It is resisted by the viscous drag created by somewhat free electrons (from the sea of electrons in metallic bonding), and by phonons. However, it is also known that shear stress from transformation drives dislocation motion. When the stress is sufficiently high, at localized barriers, it can cause surmounting a barrier or reducing its height by affecting the local bonding electrons, [65]. Hence, the bonding which is dominated by VER is a key factor in hysteresis and is affected by the chemistry of alloys through changes in VER. Separation of the effect of bonding, crystallographic, and microstructural factors on temperature hysteresis was found to be complex and not possible in current work. Temperature hysteresis requires deeper study at these scales.

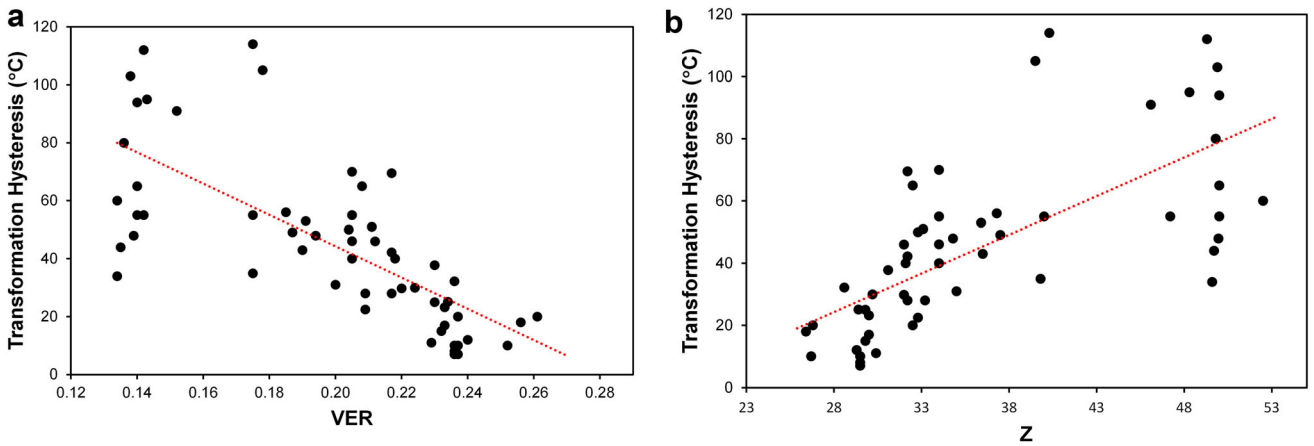

Fig. 5 Transformation temperature hysteresis vs. valence electron ratio and atomic number: variations of transformation hysteresis of TiPd- and TiPt-based alloys with **a** valence electron ratio (VER), and **b** average atomic number (Z). The dotted lines in the figure indicates the overall trends

Conclusions

The main correlations shown in this work reveal clear dependence of the transformation temperatures of TiPd- and TiPt-based alloys on the most dominant factor, i.e., valence electron ratio (VER), of these transition metal shape memory alloys. Alloying elements and in general, alloy chemistry influence the number and ratio of valence electrons of TiPd- and TiPt-based shape memory alloys and, changes the transformation temperatures through their effects on elastic properties of the crystals. M_s and A_s both significantly decrease with increasing VER from 0.134 to 0.270. This gives rise to transformation temperatures from 1184 °C (1179 °C) to 20 °C (32 °C) in these alloy systems. VER is the dominant intrinsic parameter that can be utilized to take concrete steps toward successful alloy design with the desired service temperatures. Increasing VER, and average atomic number of the alloy contribute to the widening the temperature hysteresis of the alloys. TiPd- and TiPt-based alloys with higher transformation temperatures generally show wider temperature hysteresis.

Declarations

Conflict of interest The authors declare no competing financial interests.

References

1. Concilio A, Lecce L (2015) Historical background and future perspectives. In: Lecce L, Concilio A (eds) Shape memory alloy engineering for aerospace, structural and biomedical applications. Butterworth-Heinemann Publishers, Waltham, MA, USA
2. Ostuka K, Ren X (2005) Physical metallurgy of Ti–Ni-based shape memory alloys. Prog Mater Sci 50:511
3. Zarinejad M, Liu Y, White TJ (2008) The crystal chemistry of martensite in NiTiHf shape memory alloys. Intermetallics 16:876
4. Zarinejad M, Liu Y (2008) Dependence of transformation temperatures of NiTi-based shape-memory alloys on the number and concentration of valence electrons. Adv Funct Mater 18:2789
5. Zarinejad M, Liu Y (2010) Dependence of transformation temperatures of shape-memory alloys on the number and concentration of valence electrons. In: Chen HR (ed) Shape memory alloys: manufacture, properties and applications, chapter 12. Nova Science Publishers Inc, New York
6. Planes A, Manosa L, Rioa-Jara D, Ortin J (1992) Martensitic transformation of Cu-based shape-memory alloys: elastic anisotropy and entropy change. Phys Rev B 45:7633
7. Manosa L, Jurado M, Planes A, Zarestky J, Lograsso T, Stassis C (1993) Lattice-dynamical study of the premartensitic state of the Cu–Al–Be alloys. Phys Rev B 48:15708–15711
8. Mañosa L, Jurado M, Planes A, Zarestky J, Lograsso T, Stassis C (1994) Elastic constants of bcc Cu–Al–Ni alloys. Phys Rev B 49:9969–9972
9. Ren X, Miura N, Zhang J, Otsuka K, Tanaka K, Koiwa MA (2001) A comparative study of elastic constants of Ti–Ni-based alloys prior to martensitic transformation. Mater Sci Eng A 312:196
10. Otsuka K, Wayman CM (1998) Shape memory materials. Cambridge University Press, Cambridge
11. Ren X, Taniwaki K, Otsuka K, Suzuki T, Tanaki K, Chumlyakov YI, Ueiki T (1999) Elastic constants of Ti 50 Ni 30 Cu 20 alloy prior to martensitic transformation. Philos Mag A 79:31
12. Callister WD (2007) Materials science and engineering: an introduction. Wiley, New York
13. Zarinejad M, Liu Y, Tong Y (2009) Intermetallics, transformation temperature changes due to second phase precipitation in NiTi-based shape memory alloys. Intermetallics 17:914–919
14. Quandt E, Halene C, Holleck H, Feit K, Kohl M, Smachera PS, Skokan A, Skrobanek KD (1996) Sputter deposition of TiNi, TiNiPd and TiPd films displaying the two-way shape-memory effect. Sens Actuators A 53:434
15. Schlossmacher P (1997) Microstructural investigation of a TiNiPd shape memory thin film. Mater Lett 31:119
16. Bigelow GS, Padula SAII, Garg A, Gaydosh D, Noebe RD (2010) Characterization of ternary NiTiPd high-temperature shape-memory alloys under load-biased thermal cycling. Metall Mater Trans A 41:3065
17. Zarnetta R, Savan A, Thienhaus S, Ludwig A (2007) Combinatorial study of phase transformation characteristics of a TiNiPd shape memory thin film composition spread in view of microactuator applications. Appl Surf Sci 254:743
18. Sasaki TT, Hornbuckle BC, Noebe RD, Bigelow GS, Weaver ML, Thompson GB (2013) Effect of aging on microstructure and shape memory properties of a Ni–48Ti–25Pd (At Pct) alloy. Metall Mater Trans A 44:1388
19. Rios O, Noebe R, Biles T, Garg A, Palczer A, Scheiman D, Seifert HJ, Kaufman M (2005) Characterization of ternary NiTiPt high-temperature shape memory alloys. In: SPIE conference on proceedings of smart structures and materials: behavior and mechanics. San Diego, California
20. Hoshiya T, Inoue K, Enami K (1995) Mechanical properties of TiPd-based high-temperature shape memory alloys containing Cr and Fe. In: Proceedings of the mechanical properties and phase transformations of multiphase intermetallic alloys. TMS, USA, pp 99–106.
21. Atli KC, Karaman I, Noebe RD (2014) Influence of tantalum additions on the microstructure and shape memory response of Ti50.5Ni24.5Pd25 high-temperature shape memory alloy. Mater Sci Eng A 613:250
22. Ramaiah KV, Saikrishna CN, Bhaumik SK (2013) Microstructure and transformation behaviour of $Ni_{75-X}Ti_XPd_{25}$ high temperature shape memory alloys. J Alloys Comp 554:319
23. Dezhen X, Zhou Y, Ding X, Otsuka K, Lookman T, Sun J, Ren X (2015) Ambient-temperature high damping capacity in TiPd-based martensitic alloys. Mater Sci Eng A 632:110
24. Wu KH, Liu YQ, Maich MJ, Tseng HK (1995) Mechanical properties of a NiTi–Pd high-temperature shape memory alloy. In: Proceedings SPIE smart structures and materials: smart materials, p 2189.
25. Mizuuchi K, Inoue K, Hamada K, Yamauchi K, Enami K, Sugioka M, Itami M, Okanda Y (2002) Thermomechanical behavior of Ti–25Pd–24Ni–1W shape memory alloy reinforced Ti matrix composites. Mater Sci Eng A 329–331:557
26. Benafan O, Gargb A, Noebea RD, Bigelowa GS, Padula SA II, Gaydoshc DJ, Vaidyanathand R, Clausene B, Vogel S (2015) Thermomechanical behavior and microstructural evolution of a Ni(Pd)-rich $Ni_{24.3}Ti_{49.7}Pd_{26}$ high temperature shape memory alloy. J Alloys Comp 643:275
27. Atli KC, Franco BE, Karaman I, Gaydosh D, Noebe RD (2013) Influence of crystallographic compatibility on residual strain of TiNi based shape memory alloys during thermo-mechanical cycling. Mater Sci Eng A 574:9

28. Rehman S, Khana M, Khan AN, Alia L, Jafferya SIH, Khurram M (2019) Quaternary alloying of copper with $Ti_{50}Ni_{25}Pd_{25}$ high temperature shape memory alloys. Mater Sci Eng A 763:138148
29. Ramaiah KV, Saikrishna CN, Bhaumik SK (2015) Microstructure and transformation behavior of $Ni_{24.7}Ti_{50.3}Pd_{25}$ high temperature shape-memory alloy with Sc micro-addition. Mater Charact 106:36
30. Hosoda H, Enami K, Kamio A, Inoue K (1996) Alloy design of PdTi-based shape memory alloys based on defect structures and site preference of ternary elements. J Intell Mater Syst Struct 7:312
31. Khan MI, Kim HY, Nam T, Miyazaki S (2012) Formation of nanoscaled precipitates and their effects on the high-temperature shape-memory characteristics of a $Ti_{50}Ni_{15}Pd_{25}Cu_{10}$ alloy. Acta Mater 60:5900
32. Sawaguchi T, Sato M, Ishida A (2002) Microstructure, and shape memory behavior of $Ti_{51.2}(Pd_{27.0}Ni_{21.8})$ and $Ti_{49.5}(Pd_{28.5}Ni_{22.0})$ thin films. Mater Sci Eng A 332:47
33. Mathews S, Li J, Su Q, Wuttig M (1999) Martensitic transformation in thin-film $(TiPd)_{50}$ $(TiNi)_{50}$. Philos Mag Lett 79:265
34. Kawakita M, Takahashi M, Takahashi S, Yamabe-Mitarai Y (2012) Effect of Zr on phase transformation and high-temperature shape memory effect in TiPd alloys. Mater Lett 89:336
35. Mohanchandra KP, Shin D, Carman GP (2005) Deposition and characterization of TiNiPd and TiNiPt shape memory alloy thin films. Smart Mater Struct 14:S312
36. Golberg D, Xu Y, Murakami Y, Morito S, Otsuka K (1995) Characteristics of $Ti_{50}Pd_{30}Ni_{20}$ high-temperature shape memory alloy. Intermetallics 3:35
37. Kumar PK, Desai U, Monroe JA, Lagoudas DC, Karaman I, Bigelowd G, Noebe RD (2011) Experimental investigation of simultaneous creep, plasticity, and transformation of $Ti_{50.5}Pd_{30}Ni_{19.5}$ high temperature shape memory alloy during cyclic actuation. Mater Sci Eng A 530:117
38. Ma J, Karaman I, Noebe RD (2010) High temperature shape memory alloys. Int Mater Rev 55:257
39. Noebe R, Gaydosh D, Padula S II, Garg A, Biles T, Nathal M (2005) Properties and potential of two (Ni,Pt)Ti alloys for use as high-temperature actuator materials, smart structures and materials: active materials: behavior and mechanics. In: SPIE conference proceedings, vol 5761, pp 364–375.
40. Kulinska A, Wodniecki P (2013) TiPd shape memory alloy studied by PAC method. In: Proceedings of the XLVIIIth Zakopane School of Physics, Zakopane, Poland, May 20–25
41. Matsuda H, Sato H, Shimojo M, Yamabe-Mitarai Y (2019) Improvement of high-temperature shape-memory effect by multicomponent alloying for TiPd alloys. Mater Trans 60:2282
42. Xue D, Yuan R, Xue D, Zhou Y, Zhang G, Ding X, Sun J (2018) Damping and transformation behaviors of Ti50 $(Pd_{50-x}Cr_x)$ shape memory alloys with x ranging from 4.0 to 5.0. Curr Appl Phys 18:847
43. Khachin VN, Matveeva NA, Sivokha VP, Chernov DV, Acad D (1981) High-temperature effects of shape memory in TiNi–TiPd alloys. Nauk SSSR 257:167
44. Kulinska A, Wodniecki P, Uhrmacher M (2010) Martensitic transformation in TiPd shape memory alloys studied by PAC method with ^{111}Cd probes. J Alloys Comp 494:17
45. Xu Y, Shimizu S, Suzuki Y, Otsuka K, Ueki T, Mitose K (1997) Recovery and recrystallization processes in TiPdNi high-temperature shape memory alloys. Acta Mater 45:1503
46. Kumar PK, Lagoudas DC (2010) Experimental and microstructural characterization of simultaneous creep, plasticity and phase transformation in $Ti_{50}Pd_{40}Ni_{10}$ high-temperature shape memory alloy. Acta Mater 58:1618
47. Sato H, Kim HY, Shimojo M, Yamabe-Mitarai Y (2017) Training effect on microstructure and shape recovery in Ti–Pd–Zr alloys. Mater Trans 58:1479
48. Yamabe-Mitarai Y (2020) TiPd- and TiPt-based high-temperature shape memory alloys: a review on recent advances. Metals 10:1531
49. Yamabe-Mitarai Y, Wadood A, Arockiakumar R, Hara T, Takahashi M, Takahashi S, Hosoda H (2014) High-temperature shape memory alloys based on Ti-platinum group metals compounds. Mater Sci Forum 783–786:2541
50. Yamabe-Mitarai Y (2017) Development of high-temperature shape memory alloys above 673 K. Mater Sci Forum 879:107
51. Wadood A, Yamabe-Mitarai Y (2014) Recent research and developments related to near-equiatomic titanium–platinum alloys for high-temperature applications. Platin Metals Rev 58:61
52. Canadinc D, Trehern W, Ma J, Karaman I, Sun F, Chaudhry Z (2019) Ultra-high temperature multi-component shape memory alloys. Scripta Mater 158:83
53. Yamamuro T, Morizono Y, Honjyo J, Nishida M (2006) Phase equilibrium and martensitic transformation in near equiatomic Ti–Pd alloys. Mater Sci Eng A 438–440:327
54. Todai M, Fukuda T, Kakeshita T (2013) Direction of atom displacement in incommensurate state of Ti–32Pd–18Fe shape memory alloy. Mater Lett 108:293
55. Otsuka K, Oda K, Ueno Y, Piao M, Ueki T, Horikawa H (1993) The shape memory effect in a $Ti_{50}Pd_{50}$ alloy. Script Met Mat 29:1355
56. Yamabe-Mitarai Y, Takebe W, Shimojo M (2017) Phase transformation and shape memory effect of Ti–Pd–Pt–Zr high-temperature shape memory alloys. Shap Mem Superelast 3:381
57. Wadood A, Yamabe-Mitarai Y()2014 TiAu and TiPt high temperature shape memory alloys. In: Proceedings of the 11th international Bhurban conference on applied sciences and technology (IBCAST) Islamabad, Pakistan
58. Chikosha S, Mahlatji ML, Modiba R, Chikwanda HK (2018) The effect of vanadium on structure and martensitic transformation temperature of TiPt alloy. In: IOP conference series: materials science engineering, vol 430, p 012022.
59. Wadood A, Takahashi M, Takahashi S, Hosoda H, Yamabe-Mitarai Y (2013) High-temperature mechanical and shape memory properties of TiPt–Zr and TiPt–Ru alloys. Mater Sci Eng A 564:34
60. Wadood A, Yamabe-Mitarai Y (2014) TiPt–Co and TiPt–Ru high temperature shape memory alloys. Mater Sci Eng A 601:106
61. Yamabe-Mitarai Y, Hara T, Miura S, Hosoda H (2006) Mechanical properties of Ti–50(Pt, Ir) high-temperature shape memory alloys. Mater Trans 47:650
62. Yamabe-Mitaraia Y, Arockiakumara R, Wadood A, Suresha KS, Kitashimaa T, Haraa T, Shimojoe M, Tasakia W, Takahashi M, Takahashi S, Hosoda H (2015) Ti(Pt, Pd, Au) based high temperature shape memory alloys. Mater Today Proc 2S:S517
63. Biggs T, Cortie MB, Witcomb MJ, Cornish LA (1881) Martensitic transformations, microstructure, and mechanical workability of TiPt. Metall Mater Trans A 2001:32A
64. Donkersloot HC, van Vucht JHN (1970) Martensitic transformations in gold–titanium, palladium–titanium and platinum–titanium alloys near the equiatomic composition. J Less Common Met 20:83
65. Gilman J (2003) Electronic basis of the strength of materials. Cambridge University Press, Cambridge
66. Gilman J, Cuberland RW, Kaner RB (2006) Design of hard crystals. Int J Refract Hard Mat 24:1